Research Article

Intrinsically Disordered Chromatin Protein NUPR1 Binds to the Enzyme PADI4

Salomé Araujo-Abad [1,2†], José L. Neira [1,3*†], Bruno Rizzuti [3,4], Pilar García-Morales [1], Camino de Juan Romero [1,5], Patricia Santofimia-Castaño [6*] and Juan Iovanna [6]

*1 - **IDIBE,** Universidad Miguel Hernández, 03202 Elche (Alicante), Spain*
*2 - **Centro de Biotecnología,** Universidad Nacional de Loja, Avda. Pío Jaramillo Alvarado s/n, Loja, 110111 Loja, Ecuador*
*3 - **Institute of Biocomputation and Physics of Complex Systems – Joint Unit GBsC-CSIC-BIFI,** Universidad de Zaragoza, 50018 Zaragoza, Spain*
*4 - **CNR-NANOTEC,** SS Rende (CS), Department of Physics, University of Calabria, 87036 Rende, Italy*
*5 - **Unidad de Investigación,** Fundación para el Fomento de la Investigación Sanitaria y Biomédica de la Comunidad Valenciana (FISABIO), Hospital General Universitario de Elche, Camí de l'Almazara 11, 03203 Elche (Alicante), Spain*
*6 - **Centre de Recherche en Cancérologie de Marseille,** INSERM U1068, CNRS UMR 7258, Aix-Marseille Université and Institut Paoli-Calmettes, Parc Scientifique et Technologique de Luminy, 13288 Marseille, France*

Correspondence to José L. Neira and Patricia Santofimia-Castaño: IDIBE, Edificio Torregaitán, Universidad Miguel Hernández, Avda. del Ferrocarril s/n, 03202 Elche (Alicante), Spain (J.L. Neira). Centre de Recherche en Cancérologie de Marseille, INSERM U1068, CNRS UMR 7258, Aix-Marseille Université and Institut Paoli-Calmettes, Parc Scientifique et Technologique de Luminy, 13288 Marseille, France (P. Santofimia-Castaño).*jlneira@umh.es (J. L. Neira), patricia.santofimia@inserm.fr (P. Santofimia-Castaño)*
https://doi.org/10.1016/j.jmb.2023.168033
Edited by Monika Fuxreiter

Abstract

The nuclear protein 1 (NUPR1) is an intrinsically disordered protein involved in stress-mediated cellular conditions. Its paralogue nuclear protein 1-like (NUPR1L) is p53-regulated, and its expression down-regulates that of the *NUPR1* gene. Peptidyl-arginine deiminase 4 (PADI4) is an isoform of a family of enzymes catalyzing arginine to citrulline conversion; it is also involved in stress-mediated cellular conditions. We characterized the interaction between NUPR1 and PADI4 *in vitro*, *in silico*, and *in cellulo*. The interaction of NUPR1 and PADI4 occurred with a dissociation constant of 18 ± 6 μM. The binding region of NUPR1, mapped by NMR, was a hydrophobic polypeptide patch surrounding the key residue Ala33, as pinpointed by: (i) computational results; and, (ii) site-directed mutagenesis of residues of NUPR1. The association between PADI4 and wild-type NUPR1 was also assessed *in cellulo* by using proximity ligation assays (PLAs) and immunofluorescence (IF), and it occurred mainly in the nucleus. Moreover, binding between NUPR1L and PADI4 also occurred *in vitro* with an affinity similar to that of NUPR1. Molecular modelling provided information on the binding hot spot for PADI4. This is an example of a disordered partner of PADI4, whereas its other known interacting proteins are well-folded. Altogether, our results suggest that the NUPR1/PADI4 complex could have crucial functions in modulating DNA-repair, favoring metastasis, or facilitating citrullination of other proteins.

Introduction

Peptidyl-arginine deiminases (PADI, EC 3.5.3.15), or L-arginine iminohydrolases, catalyze Ca(II)-dependent hydrolysis (deimination or citrullination) of peptidyl-arginine to peptidyl-citrulline. This post-translational modification (PTM) is irreversible and leads to the loss of a positive charge in the protein, which may cause functional alterations. The number of PADI isotypes in vertebrates increased during evolution from one in fishes and amphibians, to five human genes encoding PADI isoforms: PADI1, PADI2, PADI3, PADI4 and PADI6.[1–8] Each of these enzymes has a tissue-specific expression pattern that depends on the cell differentiation stage, and on the overall physiological or pathological conditions.[1] PADI4 was initially cloned from human myeloid leukemia HL-60 cells, after been induced by retinoic acid.[2] PADI4 is usually located in cytoplasmic granules of inflammatory cells (eosinophil, neutrophils and macrophages), mammary gland cells, stem cells, and in several tumor and metastatic tissues[9–14]; it is expressed in the cytosol and in the nucleus. Several PADI4 haplotype mutants show an increase in their enzymatic activity during apoptosis occurring *via* the mitochondrial pathway.[10] In addition, PADI4 is involved in the expression of the *p53* gene and of other *p53*-target genes,[9,15,16] as well as in p53-regulated PTMs of several proteins[17] and in p53-histone modification and alteration of the chromatin structure.[13] DNA-histone interaction is charge-dependent, and any change in the isoelectric point of a histone, including citrullination, will weaken protein–protein interactions (PPIs) involving such modified proteins.[13]

Since cancer tissues are persistently exposed to oxidative stress, activation of PADI4 in cells would possibly be related with cellular stress conditions[13]: PADI4 could work as a tumor suppressor mediating the apoptotic process in damaged cells. We have recently shown that PADI4 is a dimeric protein expressed in glioblastoma (GBM), pancreatic adenocarcinoma, and colon cancer.[18] Furthermore, PADI4 binds to importin α3 (Imp α3), a member of the armadillo (ARM) repeat-containing family of proteins, to allow its translocation into the cell nucleus,[19] and to plakophilin 1 (PKP1),[20] another protein with an ARM-repeat architecture.

NUPR1 is an 82-residue-long (8 kDa), highly basic, monomeric intrinsically disordered protein (IDP) that is overexpressed during the acute phase of pancreatitis, and in the development and regeneration of pancreas.[21] NUPR1 does not have any stable structure,[22,23] in fact, there is no evidence of transient secondary or tertiary structure along any patch in its sequence when it is isolated in solution. Furthermore, when NUPR1 binds to other macromolecules, it remains fuzzy (disordered) in the corresponding complexes.[24–27] NUPR1 binds to DNA,[24] as it happens to other chromatins, and it is involved in its repairing.[25] It is translocated into the nucleus by means of importin α3,[26,27] and possibly other importin species. It does interact with different proteins during transcription, where it is considered a crucial protein, as well as being an essential element in the stress-cell response and cell-cycle regulation, although its exact function is not known.[25,26,28–32] In all these PPIs, or in the binding to DNA, NUPR1 uses two hydrophobic regions, the so-called "hot spots", centered around residues Ala33 and Thr68.[30,31,33] The expression of the *NUPR1* gene is down-regulated by NUPR1L, a 100-residue-long NUPR1 isoform; in turn, NUPR1L expression is p53-regulated.[34] NUPR1L translocates to the nucleus of the cell, by means of a fully characterized nuclear localization signal,[35] and there it binds to DNA.[34] Threading and homology-based modelling studies suggest that NUPR1L has properties analogous to those of members of the HMG-like family of chromatin regulators. NUPR1L is an oligomeric IDP,[36] as proven by biophysical and spectroscopic methods.[37]

It has previously been shown that both NUPR1 and PADI4 are involved in stress-cell processes, sharing several regulation routes with other proteins[25,26,38–41] and intervene in the development of several types of cancer. Moreover, they share the same localization inside the cell and have complementary isoelectric points. Therefore, we hypothesized that NUPR1 and PADI4 could interact *in cellulo*. In addition, we have recently shown that the same proteins binding to NUPR1 are also capable of interacting with NUPR1L[37]; hence, in this work, we also investigated whether there was binding between NUPR1L and PADI4. To characterize the binding between PADI4 and both NUPR1 or NUPR1L, we carried out *in cellulo*, *in vitro* and *in silico* experiments. Spectroscopic techniques complemented by molecular simulations were used, while *in cellulo* assays were carried out by means of proximity ligation assay (PLA) and immunofluorescence (IF). Our hypothesis-driven experiments showed binding between these proteins both *in cellulo* and *in vitro*, with an affinity of ∼10 μM. The binding region of NUPR1 involved a hydrophobic patch surrounding the key residue Ala33 (hereafter referred to as the "30 s region"), as shown by NMR. NUPR1 remained disordered in the complex, as it occurs when it takes part in the formation of other complexes.[24–27,42] Blind molecular docking studies carried out by using the X-ray structure of PADI4[43] in interaction with all possible polypeptide patches of NUPR1 showed that the binding region involved Ala33 and its hydrophobic surroundings, as happens with other PPIs where NUPR1 is involved.[25–27,30–33] This finding was further confirmed by protein-engineering studies: the interaction with PADI4 was fully abolished *in vitro*, when mutations at Ala33 occurred. Similarly to other protein partners of NUPR1, NUPR1L was also capable of bind-

ing to PADI4, with a dissociation constant similar to that of wild-type NUPR1, as measured by fluorescence. To the best of our knowledge, NUPR1 and NUPR1L are unconventional molecular partners of PADI4, compared to its other known interacting proteins, because of their intrinsically disordered nature. Our findings suggest that NUPR1 may play a PADI4–associated function, perhaps involving the common p53-route, which may help to explain both its gene regulatory and oncogenic functions.

Results

PADI4 and NUPR1 interacted in vitro

To test whether PADI4 could bind to NUPR1 *in vitro*, we followed an experimental approach combining fluorescence, CD, and NMR, together with the use of two mutants of NUPR1 (Thr68Gln and Ala33Gln/Thr68Gln) to define the interacting region of NUPR1 involved in the binding.

Fluorescence was used to determine whether there was a change in: (i) the value of the maximum wavelength in the emission spectrum; (ii) the fluorescence intensity observed at that maximum wavelength; or (iii) both these physical parameters, when the spectrum of the complex was compared to that obtained from the addition of the spectra of the two isolated proteins. A variation in fluorescence intensity by excitation at 280 nm was observed when the complex of PADI4 with NUPR1 was formed (Figure 1 (A)), but there were no changes in the position of the maximum wavelength. Similar variations were observed by excitation at 295 nm. These findings suggest that there was binding between the two proteins, as monitored by fluorescence.

Next, we carried out far-UV CD measurements, to elucidate whether there were changes in the intensity or the shape of the addition spectrum and that of the complex. This comparison could allow us to conclude whether secondary structural changes in any of the proteins occurred when they were mixed together. The far-UV addition spectrum was identical to that of the complex (Figure 1 (B)). Since NUPR1 is an IDP, with a much smaller size than PADI4, and a spectrum typical of a random-coil conformation, with a minimum at ~200 nm[24,25] (Figure S1), our far-UV CD results can be rationalized by considering that the spectroscopic signal was mainly due to the native structure of the latter. The X-ray structure of PADI4 is composed of two domains: an immunoglobulin-like domain at the N terminus, and an α/β-propeller one (containing the active site) at the C-terminus.[43] Therefore, these findings suggest that NUPR1 remained disordered upon binding to PADI4.

To characterize the molecular bases behind the formation of the NUPR1/PADI4 complex, we sought to determine the NUPR1 regions involved in the binding. Because we have previously

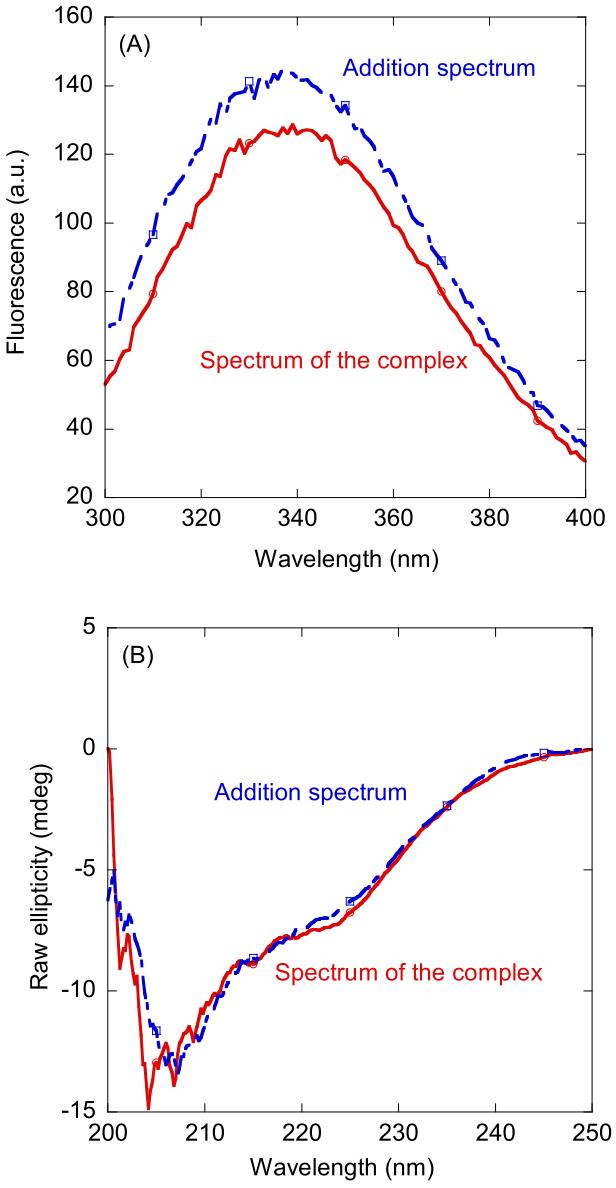

Figure 1. Binding of wild-type NUPR1 to PADI4 as monitored by spectroscopic techniques: (A) Fluorescence spectrum obtained by excitation at 280 nm of the NUPR1/PADI4 complex, and addition spectrum obtained by the sum of the spectra of the two isolated macromolecules. (B) Far-UV CD spectrum of the NUPR1/PADI4 complex, and addition spectrum obtained by the sum of the spectra of the two isolated macromolecules.

reported the NMR assignment of all residues of wild-type NUPR1[25] (Biological Magnetic Resonance Data Bank entry n. 19364), we used 2D ^{1}H-^{15}N heteronuclear single quantum correlation (HSQC) spectra of wild-type NUPR1 to monitor any possible changes in chemical shifts and/or signal intensities upon PADI4 addition. We carried out the experiments at pH 7.2, a value at which PADI4 is stable and has a native structure.[18] At this pH,

only the residues of wild-type NUPR1 most protected from solvent-exchange could be observed,[30] resulting in spectra with an unusually low number of detected signals for an 82-residue-long polypeptide chain (Figure 2). The additional presence of PADI4 in the solution resulted in no changes in the chemical shifts of the signals of the spectrum, but rather in a smaller signal intensity of the cross-peaks compared to those of the spectrum of isolated wild-type NUPR1 for residues Leu29, Tyr30 and Arg82. Furthermore, the signals of residues Ser31 and Ala33 disappeared in the presence of PADI4. This decrease in intensity, or even the complete disappearance of the cross-peaks, suggests a closer proximity of the NUPR1 residue to the enzyme. As there was no variation in the chemical shifts of any residue, it seems that NUPR1 remained disordered upon binding, confirming the results of the far-UV CD technique (Figure 1). Moreover, as there were changes only in the intensities of the cross-peak signals, the equilibrium exchange between the free and bound wild-type NUPR1 must be intermediate-to-slow within the NMR time-scale. It could be thought that the observed broadening of the signals is due, at least in part, by the change of medium viscosity due to the presence of PADI4 in solution,[44] or even by the typical difficulties faced when measuring peak intensities in HSQC spectra.[45] However, we did not observe broadening of signals in the spectra of NUPR1 while working at protein concentrations larger than 1 mM.[25] The fact that we observed the most severe broadening only in the above indicated cross-peaks suggests that such effect is specific and due to the binding of PADI4.

The results from NMR experiments suggest that the region around the 30 s of NUPR1 was involved in the binding to PADI4. The other ordinary hot spot region of NUPR1 in the interaction with its molecular partners is located around Thr68, and it contains the nuclear localization signal of NUPR1.[27] However, we could not figure out from the NMR experiments whether that region was also involved in the binding to PADI4, as it happens in the presence of other NUPR1 binding partners.[25,26,30] This region is more solvent-exposed than the 30 s portion of the sequence and, thus, the signals from residues belonging or close to that region disappeared at the pH value where the spectra were acquired. To test the importance of Thr68 in the binding to PADI4, we carried out fluorescence titration experiments of NUPR1 mutants, Thr68Gln and Ala33Gln/Thr68Gln, with PADI4. Whereas the fluorescence titration curve of the double mutant did not show a clear decrease of the fluorescence intensity as the mutant concentration was raised (Figure S2 (A)), the single mutant at position Thr68 did show a clear decrease of the intensity (Figure S2 (B); however, such variation could not be fit properly to Eq. (1). These findings with PADI4 suggest that Ala33 was a key residue in the binding to PADI4, whereas

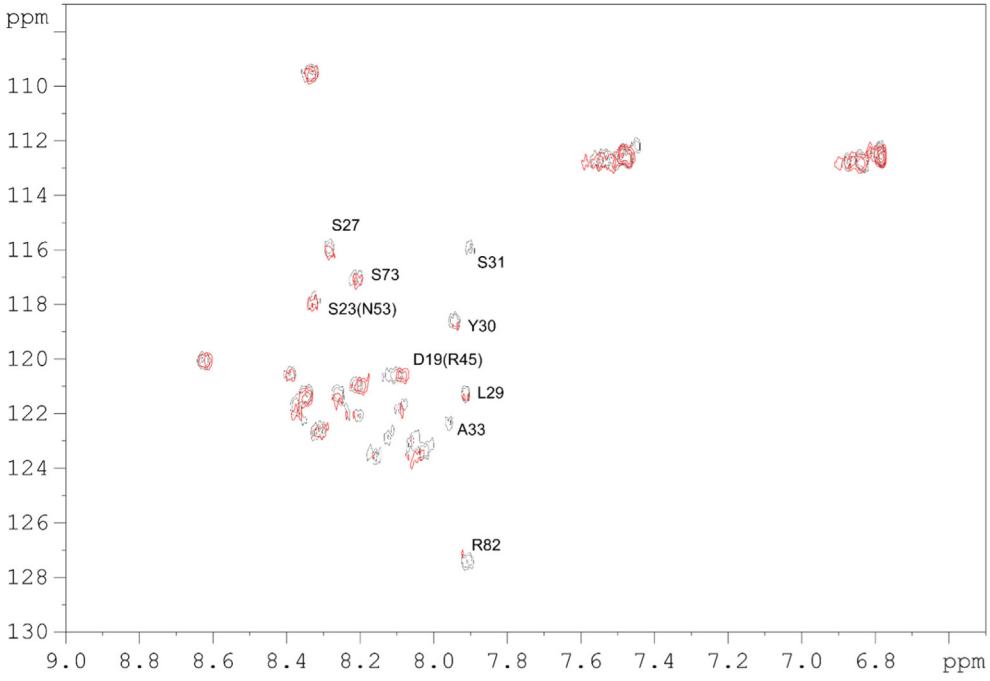

Figure 2. Interaction of wild-type NUPR1 to PADI4 mapped by 2D ^{1}H-^{15}N HSQC spectra of NUPR1: Overlay of wild-type NUPR1 spectra in the presence of 0 μM (black) and 300 μM of PADI4. Residues within parenthesis indicate signal overlapping.

removal of Thr68 resulted in a somewhat lower affinity for PADI4 than that of wild-type NUPR1 (see below), but without fully hampering the binding.

Thus, the NMR experiments further confirmed both the fluorescence and far-UV CD results, pinpointing not only the occurrence of binding, but also that such association: (i) did not alter the disordered nature of NUPR1, as shown by far-UV CD experiments; and (ii) mainly involved the 30 s region of NUPR1.

Since we observed binding between NUPR1 and PADI4, as monitored by both fluorescence and NMR, we decided to measure quantitatively such binding by using fluorescence. The titration curve yielded a dissociation constant for the complex NUPR1/PADI4 in the presence of EDTA of 18 ± 6 μM (Figure 3), and the exact same value was observed in the presence of Ca(II) (Figure S3). Thus, there were no changes in the affinity between the two proteins in the presence

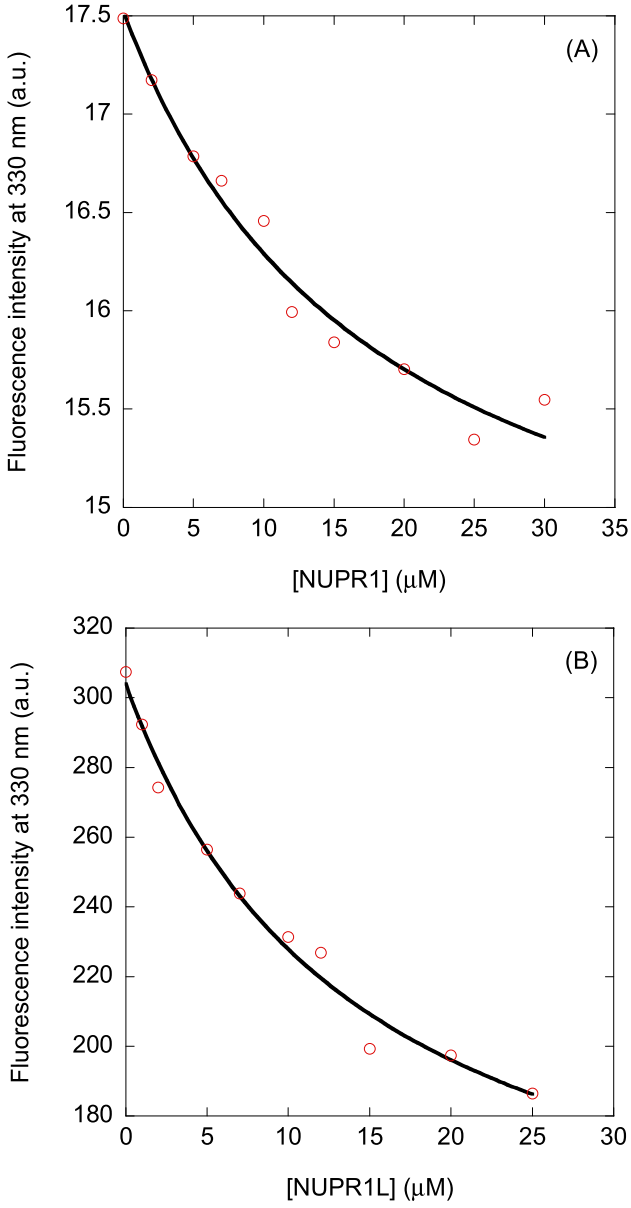

Figure 3. Measurement of the affinity of wild-type NUPR1 and NUPR1L to PADI4 as measured by fluorescence: (A) Titration curve monitoring the changes in the fluorescence at 330 nm (after excitation at 295 nm) when NUPR1 was added to PADI4 in the presence of EDTA. The fluorescence intensity is the relative signal after removal of the corresponding blank. The line through the data is the fitting to Eq. (1). (B) Titration curve monitoring the changes in the fluorescence at 330 nm (after excitation at 280 nm) when NUPR1L was added to PADI4 in the presence of EDTA. The fluorescence intensity is the relative signal after removal of the corresponding blank. The line through the data is the fitting to Eq. (2).

of the ion, and then we did not pursue any longer the investigation of the effects of Ca(II) in the binding to PADI4 of the mutants of NUPR1, or of wild-type NUPR1L. Furthermore, the binding with wild-type NUPR1 was observed to be stronger than that with the Thr68Gln mutant (Figure S2 (B)).

To sum up, NUPR1 and PADI4 interacted with an affinity constant in the low micromolar range, and the region of NUPR1 involved in the binding was mainly that around Ala33.

Computational prediction of the interaction between PADI4 and NUPR1

Molecular docking was used to obtain additional information on the binding between PADI4 and NUPR1. Because of the intrinsically unfolded structure of NUPR1, we considered the docking on the surface of PADI4 of seven-residue fragments encompassing the whole sequence of this IDP. In fact, this methodology has proved to be successful to study the binding of NUPR1 to other folded proteins[27,30,31] and to organic synthetic compounds.[46–48]

Figure 4 shows the binding affinity predicted for the various fragments, as a function of the NUPR1 sequence. The curve for wild-type NUPR1 (Figure 4, solid line) shows a global minimum in correspondence of the two seven-residue fragments centered on Asp28 and Ala33 and, therefore, overall includes the contribution of residues 25–36. The affinity was relatively favorable ($\lesssim$ –9 kcal/mol), comparable to the one predicted for the association of this region to some specific binding sites of NUPR1 molecular partners, such as the basic binding patch in the groove of the armadillo-repeat domain of PKP1.[31] A less pronounced local minimum in the curve was also visible in correspondence of residues Gln13 and Glu18, and another one around Ser58. Notably, the affinity values corresponding to residues Ala33 and Thr68 in wild-type NUPR1 both dramatically reduced (by $\sim$1 kcal/mol) upon their mutation to glutamine (Figure 4, dotted line). These results agree with our experimental findings obtained with the two NUPR1 mutants, because substitution of Ala33 fully abolished the binding to PADI4 (Figure S2 (A)), and substitution of the sole Thr68 resulted in a less favorable binding (Figure S2 (B)).

In all cases, it must be noted that the docking scores obtained in simulation should be considered as a lower limit (i.e., the affinity corresponding to the most favorable, 'ideal' case) for the actual binding energies of the NUPR1 fragments. In fact, the binding modes found for single NUPR1 fragments: (i) may not correspond to conformations easily accessible to each sequence segment when the intact polypeptide chain is considered; and (ii) the docking technique is more accurate in determining the enthalpic component of the binding, but does not consider the dynamics of the molecular system, which will likely tend to hamper the association in this case.

Despite the limitations of the simulation techniques discussed above, based on our findings, we could draw two simple but important conclusions. First, the simulation can correctly reproduce our experimental results, at least qualitatively, and contributes to pinpoint the region around the 30 s of NUPR1 sequence as the most important one for the binding to PADI4. This region is also the key hot spot for the interaction of NUPR1 with other molecular partners,[26,30,31] and this could be considered a further confirmation of the reliability of the simulation predictions. As a second conclusion, we point out that other regions of NUPR1 had a binding energy that almost

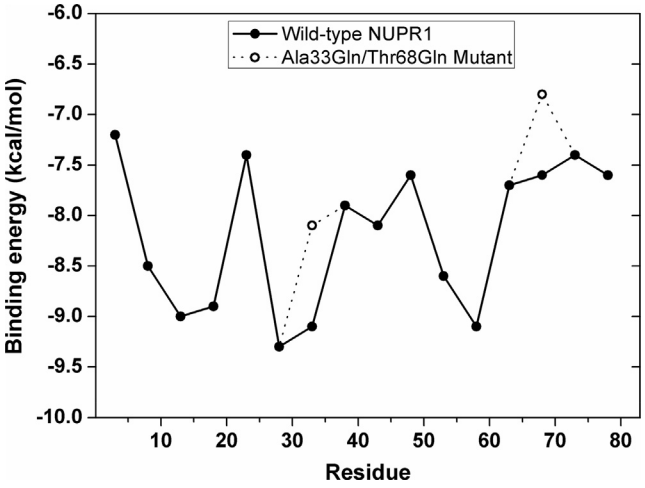

Figure 4. Predicted affinity for the binding to PADI4 of fragments of the sequence of NUPR1. The binding energy is obtained from molecular docking of seven-residue fragments performed for both wild-type NUPR1 (solid line and symbols) and the Ala33Gln/Thr68Gln protein mutant (dotted line and empty symbols).

matched that of the region around the 30 s in the interaction with the surface of PADI4, although being less favorable. In the context of a very hydrophilic and disorder-prone polypeptide chain such as NUPR1, this could be expected to result in a very dynamic and fuzzy ensemble of bound conformations of this IDP in complex with PADI4.

The most favorable docking poses obtained in simulation for the fragments of the sequence of NUPR1 were also mapped on the surface of PADI4, to identify their preferred binding locations. The results reported in Figure 5 clearly suggest the crevices at the interface of the two monomers of PADI4 as the favored region for the interaction. The docking poses were found clustered in four possible binding locations, which could be considered corresponding to two sole binding patches due to the symmetry in the structure of the PADI4 homodimer.[43] These two binding patches are at the interface between either of the two immunoglobulin-like β-structure subdomains at the N terminus, which are present in each monomer of PADI4, and the facing α-structure domain (at the C terminus) belonging to the other monomer. In particular, most of the docking poses appeared to be in contact with the immunoglobulin-like subdomains closer to the central region of PADI4. These four binding patches (or, more precisely, two couples of symmetric of patches) on the surface of PADI4 may provide a further variety of possibilities for the interaction between the two proteins.

Evidence of the interaction of NUPR1 with PADI4 in an intracellular environment

To test whether interaction between endogenous PADI4 and NUPR1 occurred within cells, we used different GBM cell lines. To perform these experiments, we used the patient-derived GBM cell lines HGUE-GB-16, HGUE-GB-18, HGUE-GB-37, HGUE-GB-39, HGUE-GB-40, HGUE-GB-42, and HGUE-GB-48.[49,50] They have been previously described to show different sensitivity/resistance profile to a variety of cancer treatments and, therefore, we hypothesized that PADI4 and NUPR1 could have different degree of association within these cell lines.[49] First, we performed IF experiments to address whether both proteins were expressed and colocalized in the same cellular compartments for the different cell lines (Figure S3). Interestingly, we found that the two proteins were highly expressed in every patient-derived cell line. Moreover, the fact that both proteins shared a nuclear staining, as shown by the colocalization with DAPI, indicates the possibility that they could interact within the nuclear compartment (Figure S3). Subsequently, we sought to confirm their interaction by using the Duolink *in situ* assay. This technique, known as PLA, resolves the binding of proteins that occurs at distances shorter than 16 Å. The green fluorescent spots, corresponding to the PLA signals, indicates that PADI4 efficiently interacted with NUPR1 within the nucleus of GBM cells (Figure 6).

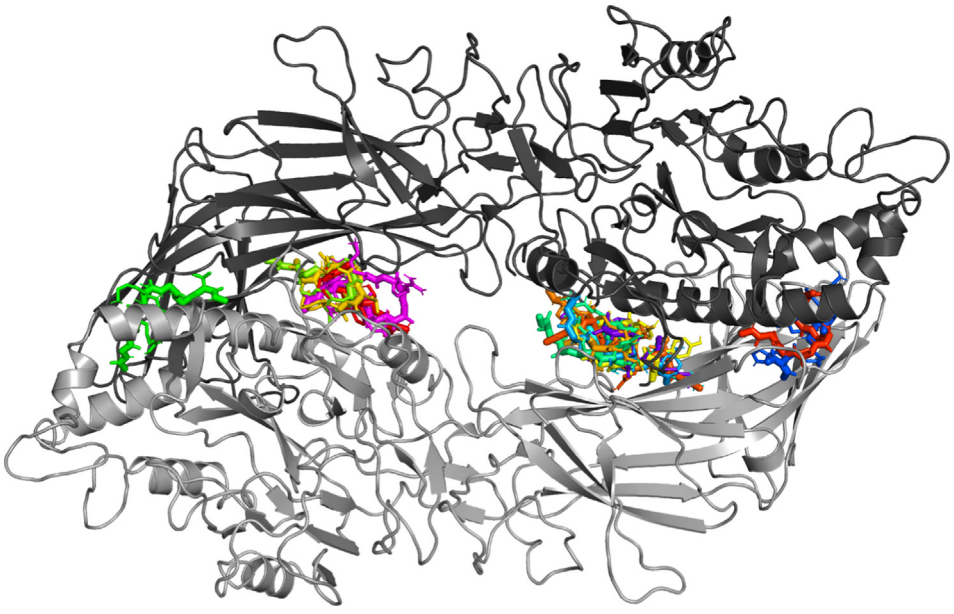

Figure 5. Predicted locations for the binding to PADI4 of fragments encompassing the sequence of NUPR1. The two monomers in the homodimer of PADI4 are represented in slightly different colors (dark and light grey). Molecular docking was performed by considering seven-residue fragments of NUPR1, overall encompassing the entire protein sequence. Fragments follow a rainbow color scheme (red → yellow → green → cyan → blue → magenta) from the N to the C terminus of NUPR1.

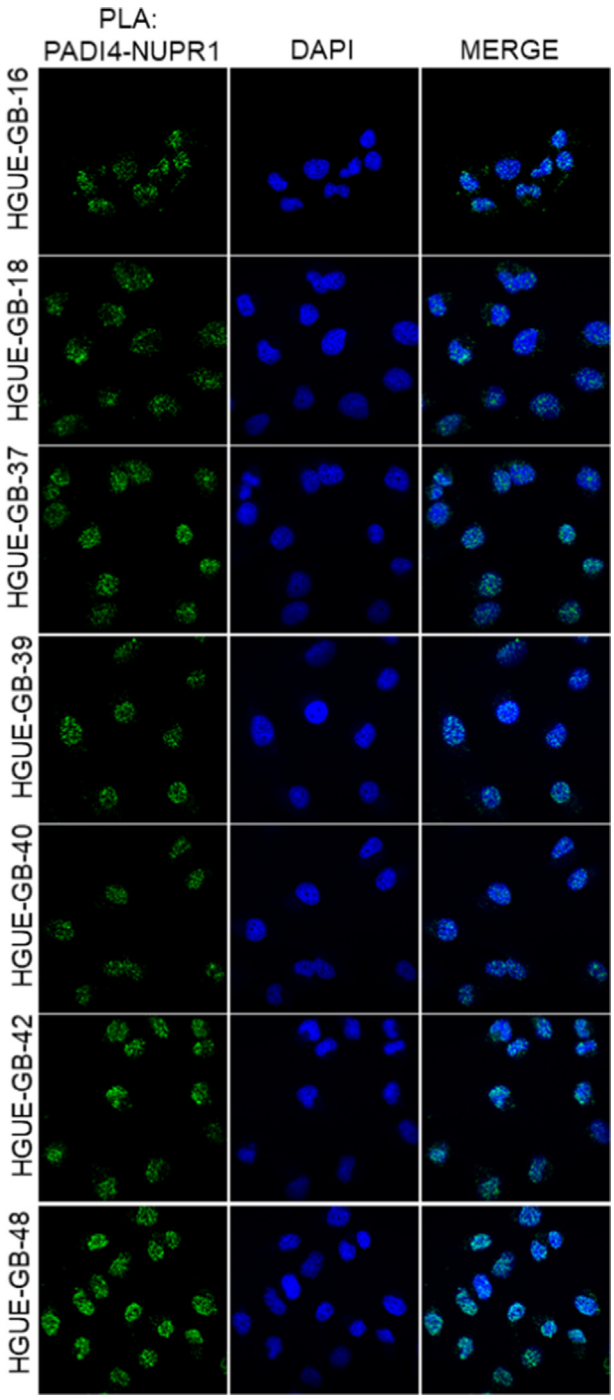

Figure 6. proximity ligation assays of PADI4 with wild-type NUPR1. Mouse anti-human PADI4 and rabbit anti-human NUPR1 were tested to reveal the interaction between the proteins in different patients-derived GBM cells.

It is important to highlight that, regardless of the patient's cell line, our results strongly indicate that PADI4 and NUPR1 are expressed, and efficiently interacted within the nuclear compartment of GBM tumor cells. As, so far, it was thought that the major role of PADI4 in the nucleus was histone citrullination, the fact that in this location it can also bind NUPR1 opens new venues to elucidate the role of both proteins in tumorigenesis.

The isoform of NUPR1, NUPR1L, also interacted with PADI4

Given that the isoform of NUPR1, i.e. NUPR1L, can interact with typical partners of NUPR1, such as prothymosin α and the C-terminal region of RING 1B,[37] we wondered whether NUPR1L could bind to PADI4, as well. As described above for NUPR1, we first performed steady-state fluores-

cence and far-UV CD experiments, and next we measured the affinity between NUPR1L and PADI4 by means of fluorescence titrations. In fact, we observed a variation in the intensity between the fluorescence spectrum of the complex and that obtained by the addition of the spectra of the isolated macromolecules (Figure 7 (A)), similar to the results for wild-type NUPR1 (Figure 1 (A)). On the other hand, conversely to what happened with NUPR1 (Figure 1 (B)), for NUPR1L the far-UV CD spectrum of the complex and that resulting from the addition of the spectra did show differences (Figure 7 (B)). Following the same reasoning applied above for NUPR1, these results suggest that, upon binding to PADI4, there was a certain degree of ordering in NUPR1L, which is also an IDP in isolation.[37] Fluorescence titrations of NUPR1L over PADI4, in the absence of Ca(II), led to an apparent dissociation constant of 14 ± 4 μM, which is similar, within the error, to that obtained for wild-type NUPR1 (Figure 3 (B)). Therefore, we can conclude that NUPR1L was also capable of binding to PADI4 *in vitro*.

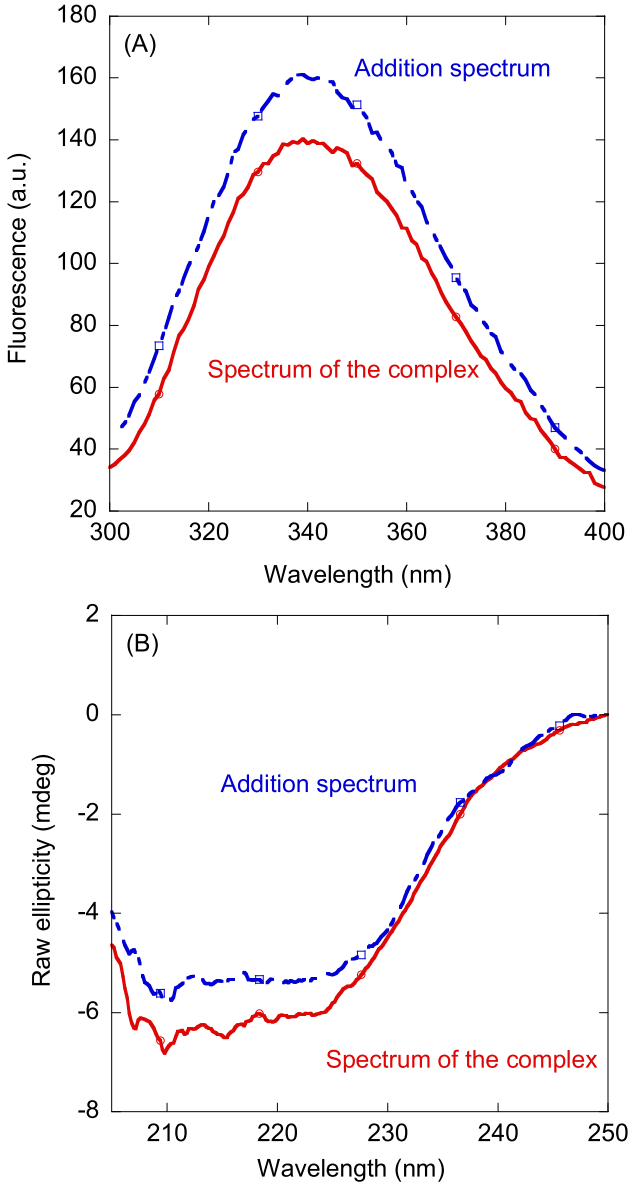

Figure 7. Binding of NUPR1L to PADI4 as monitored by spectroscopic techniques: (A) Fluorescence spectrum obtained by excitation at 280 nm of the NUPR1L/PADI4 complex, and addition spectrum obtained by the sum of the spectra of the two isolated macromolecules. (B) Far-UV CD spectrum of the NUPR1L/PADI4 complex, and addition spectrum obtained by the sum of the spectra of the two isolated macromolecules.

Discussion

NUPR1 was bound to PADI4 in vitro and in the cell

We have identified and characterized the interaction between NUPR1 and the enzyme PADI4, both being involved in stress-mediated cell responses, carcinogenesis, and cancer progression. The interaction between the two proteins was specific, as shown by two pieces of evidence: (i) the results *in cellulo* of the PLAs (Figure 4); and (ii) the findings obtained with the Thr68Gln and Ala33Gln/Thr68Gln mutants of NUPR1 *in vitro* (Figure S2). The mutations at those two specific residues decreased, or completely abolished in the case of Ala33, the interaction between NUPR1 and PADI4. The importance of residue Ala33 and of the surrounding regions of the sequence in the binding was further confirmed by the docking *in silico* of the complexes of PADI4 with wild-type NUPR1 and its mutants (Figure 4). The spectroscopic results further indicated that NUPR1 remained fuzzy in the complex formed,[42] as it happens in its other complexes either with other folded polypeptides[30–32] or with DNA.[25]

The recognition region of NUPR1 involved residues around the 30 s region in the sequence, as suggested by the NMR and protein-engineering results, and further confirmed by the docking simulations (Figures 4 and 5). The aromatic residues in this region have been previously described to intervene also in the binding to: (i) prothymosin α[33]; (ii) the C-terminal region of RING1B[30]; (iii) importin α3[26,27]; and (iv) PKP1.[31] In fact, previous molecular simulations contribute to indicate that aromatic residues in that region (Tyr30 and Tyr36) also play a role in the association to DNA[36] and in the binding of drugs designed to target NUPR1.[46–48] Not only the 30 s region of NUPR1 is a hot spot, but Thr68, as it happens in the binding with other proteins or DNA,[25–27,30,31] did also intervene in the interaction with PADI4, although it did so to a lesser extent (Figure S2). Conversely, this residue is key in the interaction with importin α3 during translocation, as its phosphorylation hampers binding to this karyopherin.[27] The fact that mutation of the sole residue Ala33 in NUPR1 can disrupt binding to another macromolecule is not unusual. A similar effect of full disruption in the binding to molecular partners by mutation of a single residue has been observed for α -synuclein[51,52] or some kinases.[53,54] In addition, our findings in this work further pinpoint that the short linear motif[55] including Ala33 was mainly responsible for the binding of NUPR1 to PADI4 (Figure 2).

Not only the intervening hot spot region, but also the measured K_d of NUPR1 for PADI4 (∼10 μM) was similar to that observed for the binding of this IDP to other proteins[25–27,30,31] and small organic compounds.[46] Such affinity is relatively small, but we believe that this low value is enough to obtain a proper control of the several regulation routes where NUPR1 intervenes,[28,29,38] achieving a high specificity despite a low affinity. Affinities in the range 1–10 μM have also been described in the formation of fuzzy complexes, involving at least an IDP that remains disordered upon binding.[42,56]

PADI4 and the NUPR1 isoform, NUPR1L, also interacted in vitro

NUPR1L is an isoform of NUPR1, and it is also an IDP, although with some evidence of residual structure. This protein is oligomeric, and capable of binding to NUPR1.[37] In contrast to what happened with NUPR1, binding of NUPR1L to PADI4 caused an ordering of the former (Figure 7 (B)), suggesting that the complex NUPR1L/PADI4 was not as disordered as that of NUPR1/PADI4. The affinity constant for PADI4 of both isoforms was similar, but it must be kept in mind that such constant for NUPR1L should include the contribution due to its self-association. Studies with other proteins capable of binding to both NUPR1L and NUPR1 have shown differences in their affinities for each isoform.[37] Conversely to what happens in the binding of NUPR1L to both prothymosin α and NUPR1,[37] it remains unclear whether its residue Trp62 was involved in the binding to PADI4, as the latter has several tryptophan residues, whose fluorescence hampers any conclusion.

Biological implications of the interaction between PADI4 and NUPR1

Although NUPR1 is an oncogene known to regulate carcinogenesis, tumorigenesis and metastasis,[38,57] it also has a suppressive function in several cancers.[38,58] On the other hand, PADI4 is activated in a large proportion of cancer tissues, probably due to citrullination of several proteins,[39,59] but it also acts as a tumor suppressor in regulating breast cancer stem cells.[60] Since both proteins can have several opposite functions (oncogene and suppression) in cancer cells, in the next paragraphs, we hypothesize how the formation of the newly-identified NUPR1/PADI4 complex, described in this work, might modulate several cell functions. Some of these hypotheses are being currently investigated in our laboratories.

PADIs catalyze the PTM of peptidyl arginine to citrulline. This citrullination reaction is a hydrolytic deamination removing the positive charge of the arginine side-chain. The human isoform PADI4 is nuclear-targeted, calcium-regulated, and it intervenes in gene regulation by citrullination of histones and in chromatin remodeling. The regions of PADI4 that are involved in the binding to NUPR1 are not yet fully experimentally identified, but based on our simulation results we predict that they are close to both the immunoglobulin-like domains and to the interface

of its two monomers. It is interesting to note that the N-terminal immunoglobulin-like domains of PADI4 have been already indicated as being involved in the binding to the p53 protein[61] and of the inhibitor growth 4 (ING4), which is also citrullinated.[62] On the other hand, NUPR1 interacted with PADI4 through the hot spot comprising residues around Ala33, and with a contribution of Thr68, as shown by NMR, site-directed mutagenesis (Figure S1 (B)), and our *in silico* results (Figure 4). NUPR1 has 9 arginine residues out of 82 amino acids, at residue number 42, 45, 48, 56, 64, 75, 78, 81, and 82. Given that NUPR1 does not contain any arginine around the 30 s, which is the main interacting region with PADI4, and Arg64 and Arg75 are close to Thr68, it seems unlikely that NUPR1 is a substrate for PADI4. However, at this stage, we cannot rule out that citrullination of NUPR1 is involved in the binding between the two proteins. We hypothesize that a possible role of NUPR1/PADI4 complex formation could be the regulation of PADI4 function. PADI4 is Ca(II)-regulated, but ion concentrations required to achieve maximal PADI4 activity are 100–1000 fold higher than those observed in activated cells. On the other hand, binding of NUPR1 could modify the conformation of the PADI4 active site, through an allosteric mechanism, in a similar fashion as the binding of Ca(II) to PADI4 does. Therefore, we can speculate that PADI's calcium dependency is altered by the interaction with NUPR1. Along this hypothesis, antibodies isolated from patients with rheumatoid arthritis might bind and activate PADI4 by lowering the Ca(II) concentration required for its maximal activity.[63]

The mechanisms that regulate PADI4 function and how it works within cells remain unclear.[40,41] It is known that estrogen regulates the expression of PADI4 through both the classical and non-classical pathways.[64] It has also been reported that p53 transactivates PADI4 through a *p53*-binding site at the first intron.[15] Moreover, the significance of PADI4-mediated protein citrullination in the p53-signaling pathway has been proved by attenuating p53-mediated growth-inhibitory activity after the knockdown PADI4 expression.[17] PADI4 is involved in the repression of p53-target genes by interacting with the C-terminus of p53, as well as having other modulation effects on p53-target genes.[15,16] As PADI4 has histone-deiminase activity, it results in the negative regulation of downstream p53-target genes, and thus PADI4 functions as a p53 co-repressor. Moreover, NUPR1L is also p53-regulated, and its expression down-regulates that of the *NUPR1* gene, leading to binding to NUPR1. We suggest that the formation of the complex NUPR1/PADI4 might avoid the repression of p53 and, in addition, hampering the binding of NUPR1 by its own isoform.

In response to DNA damage, histones H3 and H4 are citrullinated by PADI4, which in turn promotes DNA fragmentation.[13] In addition, DNA damage triggers the formation of a complex between NUPR1 and the male specific lethal protein (MSL).[25,65] The NUPR1/MSL complex protects cells from death. The possibility of forming a complex NUPR1/PADI4 might hamper the activation of the two DNA-repair routes, and thus it could be a way of modulating such repair.

The role of NUPR1 in cancer progression was identified in the study of breast metastasis from breast cancer.[66] This study has shown that expression of NUPR1 allows one to discern between metastatic-potential breast cancer cells and those without such potential; that is, NUPR1 is necessary for the establishment of cells derived from breast cancer cells in a secondary organ. Citrullination of glycogen synthase kinase-3β (GSK-3β) by PADI4 induces epithelial-to-mesenchymal transition in breast cancer cells,[67] which is a key step in breast cancer cells to achieve metastasis in other organs. We suggest that the presence of NUPR1, and formation of its complex with PADI4, might hamper the citrullination of GSK-3 β,and therefore would decrease the epithelial-to-mesenchymal transition in breast cancer cells.

Altogether, then, our results demonstrate the interaction between PADI4 with NUPR1 and NUPR1L, and they might highlight the importance of this complex in tumorigenesis and shed some light in the possible regulation mechanisms of these proteins.

Materials and methods

Materials

Imidazole, Trizma base and acid, DNase, SIGMAFAST protease tablets, NaCl and Ni(II)-resin, were from Sigma (Madrid, Spain). Isopropyl-β-D-1-thiogalactopyranoside, kanamycin and ampicillin were obtained from Apollo Scientific (Stockport, UK). Dialysis tubing with a molecular weight cut-off of 3500 Da, Triton X-100, TCEP (Tris(2-carboxyethyl)phosphine) and the SDS protein marker (PAGEmark Tricolor) were from VWR (Barcelona, Spain). Amicon centrifugal devices with a molecular weight cut-off of 30 kDa or 3 kDa were from Millipore (Barcelona, Spain). The rest of the materials used were of analytical grade. Water was deionized and purified on a Millipore system.

Protein expression and purification

PADI4, NUPR1 and NUPR1L were purified as previously described.[18–20,24,25,37] Protein concentrations were determined by UV absorbance, employing an extinction coefficient at 280 nm estimated from the number of tyrosines (in particular, NUPR1 has only two tyrosine residues) and tryptophans in each protein.[68]

Fluorescence

Steady-state fluorescence. A Cary Varian spectrofluorometer (Agilent, Santa Clara, CA, USA), interfaced with a Peltier unit, was used to collect fluorescence spectra at 25 °C, by excitation at either 280 or 295 nm. The other experimental details have been described elsewhere.[69] Appropriate blank corrections corresponding to curves obtained for samples containing only buffers were made in all spectra. Following the standard protocols used in our laboratories, the samples were prepared the day before and left overnight at 5 °C; before experiments, samples were left for 1 h at 25 °C. A 1-cm path length quartz cell (Hellma, Kruibeke, Belgium) was used. Concentration of PADI4 was 2 μM (in protomer units) and those of NUPR1 or NUPR1L were 20 μM (in protomer units for the latter). Experiments were performed in 20 mM Tris buffer (pH 7.5), 5 mM TCEP, 150 mM NaCl, 10 mM EDTA and 5 % glycerol, in triplicates with newly prepared samples. Variations of results among the experiments were lower than 5 %.

Binding experiments of PADI4 with wild-type NUPR1. For the titration of wild-type NUPR1 with PADI4, increasing amounts of monomeric NUPR1, in the concentration range 0–30 μM, were added to a solution with a fixed concentration of PADI4 (2 μM, in protomer units). Experiments were carried out in the buffer described above, with the same experimental set-up; experiments were also carried out in the presence of buffer, without EDTA and with 10 mM Ca(II). In all cases, the appropriate blank corrections with solutions containing only the corresponding amount of NUPR1 were applied. Spectra were corrected for inner-filter effects.[70] The titration was repeated three times, using new samples. In the three cases, the variations in the results were lower than 10 %.

The dissociation constant of the complex, K_d, was calculated by fitting the binding isotherm obtained by plotting the observed fluorescence change as a function of NUPR1 concentration to a general binding model, explicitly considering ligand depletion in solution[71,72]:

$$F = F_0 + \frac{\Delta F_{max}}{2[PADI4]_T}\left([NUPR1]_T + [PADI4]_T + K_d\right) - \sqrt{\left(\left([NUPR1]_T + [PADI4]_T + K_d\right)^2 - 4[NUPR1]_T[PADI4]_T\right)} \quad (1)$$

where F is the measured fluorescence of the solution with the fixed PADI4 concentration (2 μM, in protomer units) and a given value for NUPR1, after subtraction of the corresponding blank with the same concentration of the latter; ΔF_{max} is the largest change in the fluorescence of NUPR1 when saturation was reached, compared to the fluorescence of each isolated chain; F_0 is the fluorescence intensity when no NUPR1 was added; $[PADI4]_T$ is the constant, total concentration of PADI4 (2 μM, in protomer units); and $[NUPR1]_T$ is that of NUPR1, which was varied during the titration. Fitting to Eq. (1) was carried out by using KaleidaGraph (Synergy software, Reading, USA).

Binding experiments of PADI4 with NUPR1 mutants. For the titration of mutants with PADI4, increasing amounts of either the single mutant Thr68Gln or the double mutant Ala33Gln/Thr68Gln of NUPR1, in the concentration range 0–30 μM, were added to a solution with a fixed concentration of PADI4 (2 μM, in protomer units). Experiments were carried out as described for wild-type NUPR1, with the same experimental set-up, in the presence of 10 mM EDTA.

Binding experiments of PADI4 with NUPR1L. For the titration of NUPR1L with PADI4, increasing amounts of NUPR1L species, in the concentration range 0–25 μM, were added to a solution with a fixed concentration of PADI4 (2 μM, in protomer units). Experiments were carried out in the buffer described above, with the same experimental set-up, in the presence of 10 mM EDTA. In all cases, the appropriate blank corrections by using spectra obtained for solutions containing only the corresponding amount of NUPR1L were applied. Spectra were corrected for inner-filter effects.[70] The titration was repeated three times, using new samples. In the three cases, the variations in the results were lower than 10 %.

The dissociation constant of the complex, K_d, was calculated by fitting the binding isotherm obtained by plotting the observed fluorescence change as a function of NUPR1L concentration to a general binding model, explicitly considering ligand depletion in solution[71,72]:

$$F = F_0 + \frac{\Delta F_{max}}{2[PADI4]_T}\left([NUPR1L]_T + [PADI4]_T + K_d\right) - \sqrt{\left(\left([NUPR1L]_T + [PADI4]_T + K_d\right)^2 - 4[NUPR1L]_T[PADI4]_T\right)} \quad (2)$$

where the symbols in Eq. (2) have the same meaning as those in Eq. (1). However, it is important to indicate that the K_d obtained from Eq. (2) was an apparent dissociation constant, as NUPR1L is an oligomer with a self-dissociation in the order of nM.[37]

Circular dichroism (CD)

Far-UV CD spectra were collected on a Jasco J810 spectropolarimeter (Jasco, Tokyo, Japan) with a thermostated cell holder and interfaced with a Peltier unit. The instrument was periodically calibrated with (+)-10-camphorsulfonic acid. A 0.1-cm path length cell was used (Hellma, Kruibeke, Belgium). All spectra were corrected by subtracting the corresponding baseline. Concentration of each polypeptide (wild-type NUPR1, NUPR1L, or PADI4) and the buffers used

were the same used for fluorescence experiments. We could not obtain meaningful data below ~200 nm, for any of the two proteins, due to the absorbance of the components of the buffer (Figure S1). Samples were prepared the day before and left overnight at 5 °C to allow them to equilibrate. Before starting the experiments, samples were further left for 1 h at 25 °C. Isothermal wavelength spectra of each isolated macromolecule (at 25 °C) and those of the corresponding complex (NUPR1/PADI4 or NUPR1L/PADI4) were acquired as an average of 6 scans, at a scan speed of 50 nm/min, with a response time of 2 s and a band-width of 1 nm.

Nuclear Magnetic Resonance (NMR)

The NMR experiments were performed on a Bruker Avance DRX-500 spectrometer (Karlsruhe, Germany) equipped with a triple resonance probe and *z*-pulse field gradients. Spectra were acquired at 25 °C and pH 7.2 (Tris, 50 mM); probe temperature was calibrated with a methanol NMR standard.[73] It is important to indicate here that the buffer employed in the NMR experiments is slightly different to that used in the far-UV CD and fluorescence experiments, to increase the signal-to-noise ratio in the spectra (which would deteriorate in the presence of high NaCl concentration, EDTA, TCEP and glycerol).

The cross-peaks in the 2D ^{1}H-^{15}N HSQC NMR spectra[74] of NUPR1 were identified by using previously determined assignments at pH 4.5.[25] We did not carry out the study of the binding between NUPR1 and PADI4 at this pH value, because the latter precipitates at acidic conditions.[18] The number of signals observed in the 2D ^{1}H-^{15}N HSQC NMR spectra at pH $\geq$ 7.0 dramatically decreased when compared to low pH due to hydrogen-exchange at physiological conditions, as it has been observed when exploring binding to other partners[30,31,75] (see also Results section).The sample containing the mixture of NUPR1 and PADI4 was prepared by using Amicon centrifugal devices of 3 kDa cut-off, where both proteins were initially mixed at dilute concentrations in buffer in 20 mM Tris (pH 7.5), 5 mM TCEP, 150 mM NaCl, 10 mM EDTA and 5 % glycerol, and then concentrated and exchanged to deuterated Tris buffer, used in NMR experiments.

Spectra were acquired in the TPPI (time proportional phase increment) mode. The concentration of ^{15}N-labeled NUPR1 was 100 μM either in isolation or in the presence of 300 μM of PADI4. The spectra were typically acquired with 2,048 complex points in the ^{1}H dimension, 60 complex points in the ^{15}N dimension, with 32 or 64 scans. Typical spectral widths for the 2D ^{1}H-^{15}N HSQC NMR spectra were 6,000 (^{1}H) and 1,500 (^{15}N) Hz. The resulting matrix of each experiment was zero-filled to double the number of original points in all dimensions, and shifted squared sine-bell apodization functions were applied before Fourier transformation. NMR data were processed and analyzed using TopSpin 1.3 (Bruker, Karlsruhe, Germany). Signal intensities in the two NMR spectra (of isolated NUPR1, and in the presence of PADI4) were measured, and in each experiment, intensities were corrected by the corresponding value of the receiver gain. Spectra were calibrated with external TSP for ^{1}H and for the indirect dimensions, as previously described.[73]

Molecular docking

Molecular docking was used to study the binding of PADI4 and NUPR1 in a simplified way, because of the relatively large size of PADI4 (a homodimer with 663 residues in each monomer) and, more importantly, the intrinsically unfolded character of NUPR1 (an 82-residue-long fully disordered sequence). The structure of PADI4 was built on the basis of the X-ray diffraction model deposited in the Protein Data Bank (PDB entry: 3APN.[43] The binding affinity towards PADI4 was predicted by considering seven-residue fragments encompassing in total the whole sequence of NUPR1, following the same protocol we adopted in other previous works.[30,31,27,76] The fragments were capped at the N- and C-terminal endings by using an acetyl and amide moiety, respectively – with the exceptions of the protein termini, where the $-NH_3^+$ and $-COO^-$ groups were preserved.

The simulations were performed by using the docking engine AutoDock Vina, version 1.1.2.[77] Apolar hydrogen atoms were subsumed in the carbon atoms they are attached to, whereas polar hydrogens were explicitly considered for both the docking host protein PADI4 and the guest fragments of NUPR1. A blind exploration was carried out with an exhaustiveness twice larger with respect to the default value.[78] The search volume was centered on the PADI4 homodimer and had the size of 110 Å × 70 Å × 110 Å, which was enough to include the whole protein surface. Full flexibility due to rotations around each dihedral angle was guaranteed to the NUPR1 fragments.

Cell lines

Isolation of the seven, primary human GBM cell lines (HGUE-GB-16, HGUE-GB-18, HGUE-GB-37, HGUE-GB-39, HGUE-GB-40, HGUE-GB-42 and HGUE-GB-48) was performed from surgical washes, as reported previously.[49] GBM cells were cultured in Dulbecco's Modified Eagle's Medium: Nutrient Mixture F-12 (DMEM F-12) (Gibco, New York, USA), supplemented with 10 % (v/v) heat-inactivated fetal bovine serum (FBS) (HyClone/Cytiva, Little Chalfont, UK) and 1 % (v/v) penicillin/streptomycin mixture (Biowest, Bradenton, USA). Cells were incubated at 37 °C in a humidified 5 % CO_2 atmosphere as previously described.[49,50]

Immunofluorescence (IF)

An amount of 40,000 GBM cells were seeded in twenty-four-well plates on coverslips.[25,30] After fixation, cells were incubated with a mouse anti-PADI4 (1:200, mouse; Abcam, Cambridge, UK) primary antibody and anti-NUPR1 antibody (1:100, rabbit; homemade). After washing out the first antibody, cells were incubated with Alexa Fluor 568-labeled anti-mouse (1:500) and Alexa Fluor 488-labeled anti-rabbit (1:500) secondary antibodies (Invitrogen, Barcelona, Spain) and DAPI (4′,6-diamidino-2-phenylindole, Thermo Fisher Scientific, Valencia, Spain) was used to stain the nucleus. Image acquisition was carried out by using a confocal microscope LSM 880 (×63 lens) controlled by Zeiss Zen Black (Zeiss, Oberkochen, Germany).

proximity ligation assay (PLA)

An amount of 40,000 GBM cells of each patient were seeded in twenty-four-well plates on coverslips. Cells were assayed 24 h later. Cells were washed twice in phosphate buffer solution (PBS), fixed, washed twice again, permeabilized in PBS/0.2 % Triton X-100, and saturated with blocking solution for 30 min before immunostaining with Duolink by using PLA Technology (Merck, Madrid, Spain), following the manufacturer's protocol. Anti-PADI4 and anti-NUPR1 primary antibodies were used. Then, slides were processed for *in situ* PLA by using sequentially the Duolink In Situ Detection Reagents Green, Duolink In Situ PLA Probe Anti-Mouse MINUS, and Duolink In Situ PLA Probe Anti-Rabbit PLUS (Merck, Madrid, Spain). In these experiments, green fluorescence corresponds to the PLA-positive signal, and it indicates that the two proteins are bound to form a complex. Blue fluorescence corresponds to nuclei (so-called DAPI staining). To check the specificity of the PLA signal, negative control experiments omitting one of the primary antibodies and positive controls[25,30] were performed. Image acquisition was carried out by using the same confocal microscope described above.

Funding

This research was funded by Instituto de Salud Carlos III and European Union (ERDF/ESF, "Investing in your future") [CP19/00095 to CdJ] [PI22/00824 to CdJ]; and Consellería de Innovación, Universidades, Ciencia y Sociedad Digital (Generalitat Valenciana) [CAICO 2021/0135 to CdJ and JLN]. SAA was recipient of a "Carolina Foundation predoctoral fellowship 2020". SAA was supported by the Company of Biologists Ltd to travel to the laboratory of JLI and PSC (grant number DMMTF2110601). The funders had no role in the study design, data collection and analysis, decision to publish, or preparation of the manuscript.

CRediT authorship contribution statement

Salomé Araujo-Abad: Investigation, Formal analysis, Writing – review & editing. **José L. Neira:** Conceptualization, Methodology, Investigation, Formal analysis, Writing – original draft, Resources, Writing – review & editing, Funding acquisition. **Bruno Rizzuti:** Conceptualization, Methodology, Investigation, Formal analysis, Writing – original draft, Writing – review & editing. **Pilar García-Morales:** Resources, Writing – review & editing. **Camino de Juan Romero:** Conceptualization, Writing – original draft, Resources, Writing – review & editing, Funding acquisition. **Patricia Santofimia-Castaño:** Conceptualization, Methodology, Investigation, Formal analysis, Writing – original draft, Resources, Writing – review & editing, Funding acquisition. **Juan Iovanna:** Conceptualization, Methodology, Writing – review & editing, Funding acquisition.

DATA AVAILABILITY

Data will be made available on request.

DECLARATION OF COMPETING INTEREST

The authors declare that they have no known competing financial interests or personal relationships that could have appeared to influence the work reported in this paper.

Acknowledgment

BR acknowledges the kind use of computational resources of the European Magnetic Resonance Center (CERM), Sesto Fiorentino (Florence), Italy.

Appendix A. Supplementary Data

The supplementary material contains: far-UV CD spectra of isolated NUPR1 and PADI4 in 20 mM Tris buffer (pH 7.5), 5 mM TCEP, 150 mM NaCl, 10 mM EDTA and 5 % glycerol (Figure S1); fluorescence titration curves for Thr68Gln and Ala33Gln/Thr68Gln mutants of NUPR1 in the presence of PADI4 and 10 mM EDTA (Figure S2); fluorescence titration curve of wild-type NUPR1 when added to PADI4 in the presence of 10 mM Ca(II) (Figure S3); IF experiments on PADI4 with NUPR1 in several patient-derived cell lines (Figure S4). Supplementary data to this article can

be found online at https://doi.org/10.1016/j.jmb.2023.168033.

Received 27 November 2022;
Accepted 21 February 2023;
Available online 27 February 2023

Keywords:
PADI4;
protein–protein interactions;
citrullination;
fluorescence;
molecular modeling

† These two authors contributed equally to this work.

Abbreviations:
CD, circular dichroism; DAPI 4′, 6-diamidino-2-phenylindole; GBM, glioblastoma; GSK-3β, glycogen synthase kinase-3β; HSQC, heteronuclear single quantum correlation; IDP, intrinsically disordered protein; IF, immunofluorescence; Impα3, human importin α3 protein; MSL, male specific lethal protein; NUPR1, nuclear protein 1; NUPR1L, nuclear protein 1-like, isoform of NUPR1; PADI, peptidyl-arginine deiminase; PBS, phosphate buffer solution; PDB, Protein Data Bank; PKP1, plakophilin 1; PLA, proximity ligation assay; PPI, protein–protein interaction; PTM, post-translational modification; UV, ultraviolet

References

1. Vossenaar, E.R., Zendman, A.J.W., van Venrooij, W.J., Pruijn, G.J.M., (2003). PAD, a growing family of citrullinating enzymes: genes, features and involvement in disease. *Bioessays* **25**, 1106–1118. https://doi.org/10.1002/bies.10357.
2. Nakashima, K., Hagiwara, T., Ishigami, A., Nagata, S., Asaga, H., Kuramoto, M., Senshu, T., Yamada, M., (1999). Molecular characterization of peptidylarginine deiminase in HL-60 cells induced by retinoic acid and 1alpha,25-dihydroxyvitamin D(3). *J. Biol. Chem.* **274**, 27786–122792. https://doi.org/10.1074/jbc274.39.27786.
3. Guerrin, M., Ishigami, A., Méchin, M.C., Nachat, R., Valmary, S., Sebbag, M., Simon, M., Senshu, T., et al., (2003). cDNA cloning, gene organization and expression analysis of human peptidylarginine deiminase type I. *Biochem. J.* **370**, 167–174. https://doi.org/10.1042/bj20020870.
4. Ishigami, A., Ohsawa, T., Asaga, H., Akiyama, K., Kuramoto, M., Maruyama, N., (2002). Human peptidylarginine deiminase type II: molecular cloning, gene organization, and expression in human skin. *Arch. Biochem. Biophys.* **407**, 25–31. https://doi.org/10.1016/s0003-9861(02)00516-7.
5. Kanno, T., Kawada, A., Yamanouchi, J., Yosida-Noro, C., Yoshiki, A., Shiraiwa, M., Kusakabe, M., Manabe, M., et al., (2000). Human peptidylarginine deiminase type III: Molecular cloning and nucleotide sequence of the cDNA, properties of the recombinant enzyme, and immunohistochemical localization in human skin. *J. Invest. Dermatol.* **115**, 813–823. https://doi.org/10.1046/j.1523-1747.2000.00131.x.
6. Chavanas, S., Méchin, M.C., Takahara, H., Kawada, A., Nachat, R., Serre, G., Simon, M., (2004). Comparative analysis of the mouse and human peptidylarginine deiminase gene clusters reveals highly conserved non-coding segments and a new human gene, PADI6. *Gene* **330**, 19–27. https://doi.org/10.1016/j.gene.2003.12.038.
7. Hriria, H., Mokrab, Y., Mizuguchi, K., (2006). The guanidino-group modifying enzymes: structural basis for their diversity and commonality. *Proteins* **64**, 1010–1023. https://doi.org/10.1002/prot.20863.
8. Dong, S., Kanno, T., Yamaki, A., Kojima, T., Shiraiwa, M., Kawada, A., Méchin, M.C., Chavanas, S., et al., (2006). NF-Y and Sp1/Sp3 are involved in the transcriptional regulation of the peptidylarginine deiminase type III gene (PADI3) in human keratinocytes. *Biochem. J.* **397**, 449–459. https://doi.org/10.1042/BJ20051939.
9. Yang, C., Dong, Z.-Z., Zhang, J., Teng, D., Luo, X., Li, D., Zhou, Y., (2021). Peptidylarginine deiminases 4 as a promising target in drug discovery. *Eur. J. Med. Chem.* **226**, https://doi.org/10.1016/j.ejmech.2021.113840 113840.
10. Slade, D.J., Horibata, S., Coonrod, S.A., Thompson, P.R., (2014). A novel role for protein arginine deiminase 4 in pluripotency: the merging role of citrullinated histone H1 in cellular programming. *Bioessays* **36**, 736–740. https://doi.org/10.1002/bies.201400057.
11. Witalison, E.E., Thompson, P.R., Hofseth, L.J., (2015). Protein arginine deiminases and associated citrullination: physiological functions and diseases associated with dysregulation. *Curr. Drug Targets* **16**, 700–710. https://doi.org/10.2174/1389450116666150202160954.
12. Wang, Y., Chen, R., Gan, Y., Ying, S., (2021). The roles of PAD2- and PAD4-mediated protein citrullination catalysis in cancers. *Int. J. Cancer* **148**, 267–276. https://doi.org/10.1002/ijc.33205.
13. Tanikawa, C., Espinosa, M., Suzuki, A., Masuda, K., Yamamoto, K., Tsuchiya, E., Ueda, K., Daigo, Y., et al., (2012). Regulation of histone modification and chromatin structure by the p53-PADI4 pathway. *Nat. Commun.* **3**, 676. https://doi.org/10.1038/ncomms1676.
14. Chang, X., Han, J., Pang, L., Zhao, Y., Yang, Y., Shen, Z., (2009). Increased PADI4 expression in blood and tissues of patients with malignant tumors. *BMC Cancer* **9**, 40. https://doi.org/10.1186/1471-2407-9-40.
15. Li, P., Yao, H., Zhang, Z., Li, M., Luo, Y., Thompson, P.R., Gilmour, D.S., Wang, Y., (2008). Regulation of p53 target gene expression by peptidylarginine deiminase 4. *Mol. Cell Biol.* **28**, 4745–4758. https://doi.org/10.1128/MCB.01747-07.
16. Li, P., Wang, D., Yao, H., Doret, P., Hao, G., Shen, Q., Qiu, H., Zhang, X., et al., (2010). Coordination of PAD4 and HDAC2 in the regulation of p53-target gene expression. *Oncogene* **29**, 3153–3162. https://doi.org/10.1038/onc.2010.51.
17. Tanikawa, C., Ueda, K., Nakagawa, H., Yoshida, N., Nakamura, Y., Matsuda, K., (2009). Regulation of protein citrullination through p53/PADI4 network in DNA damage response. *Cancer Res.* **69**, 8761–8769. https://doi.org/10.1158/0008-5472.CAN-09-2280.
18. Neira, J.L., Araujo-Abad, S., Cámara-Artigas, A., Rizzuti, B., Abián, O., Giudici, A.M., Velázquez-Campoy, A., de Juan Romero, C., (2022). Biochemical and biophysical

characterization of PADI4 supports its involvement in cancer. *Arch. Biochem. Biophys.* **717**, https://doi.org/10.1016/j.abb.2022.109125 109125.
19. Neira, J.L., Rizzuti, B., Abián, O., Araujo-Abad, S., Velázquez-Campoy, A., de Juan Romero, C., (2022). Human enzyme PADI4 binds to the nuclear carrier Importin α3. *Cells* **11**, 2166. https://doi.org/10.3390/cells11142166.
20. Neira, J.L., Rizzuti, B., Araujo-Abad, S., Abian, O., Fárez-Vidal, M.E., Velazquez-Campoy, A., de Juan Romero, C., (2022). The armadillo-repeat domain of Plakophilin 1 binds to human enzyme PADI4. *Biochim. Biophys. Acta Proteins Proteom.*. https://doi.org/10.1016/j.bbapap.2022.140868.
21. Mallo, G.V., Fiedler, F., Calvo, E.L., Ortiz, E.M., Vasseur, S., Keim, V., Morisset, J., Iovanna, J.L., (1997). Cloning and expression of the rat p8 cDNA, a new gene activated in pancreas during the acute phase of pancreatitis, pancreatic development, and regeneration, and which promotes cellular growth. *J. Biol. Chem.* **272**, 32360–32369. https://doi.org/10.1074/jbc.272.51.32360.
22. Uversky, V.N., (2013). A decade and a half of protein intrinsic disorder: biology still waits for physics. *Protein Sci.* **22**, 693–724. https://doi.org/10.1002/pro.2261.
23. Wright, P.E., Dyson, H.J., (2015). Intrinsically disordered proteins in cellular signaling and regulation. *Nat. Mol. Cell Biol.* **16**, 18–29. https://doi.org/10.1038/nrm3920.
24. Encinar, J.A., Mallo, G.V., Mizyrycki, C., Giono, L., González-Ros, J.M., Rico, M., Cánepa, E., Moreno, S., et al., (2001). Human p8 is a HMG-I/Y-like protein with DNA binding activity enhanced by phosphorylation. *J. Biol. Chem.* **276**, 2742–2751. https://doi.org/10.1074/jbc.M008594200.
25. Aguado-Llera, D., Hamidi, T., Doménech, R., Pantoja-Uceda, D., Gironella, M., Santoro, J., Velázquez-Campoy, A., Neira, J.L., et al., (2013). Deciphering the binding between Nupr1 and MSL1 and their DNA-repairing activity. *PLoS One* **8**, e78101. https://doi.org/10.1371/journal.pone.0078101.
26. Lan, W., Santofimia-Castaño, P., Swayden, M., Xia, Y., Zhou, Z., Audebert, S., Camoin, L., Huang, C., et al., (2020). ZZW-115-dependent inhibition of NUPR1 nuclear translocation sensitizes cancer cells to genotoxic agents. *JCI Insight* **5**, e138117. https://doi.org/10.1172/jci.insight.138117.
27. Neira, J.L., Rizzuti, B., Jiménez-Alesanco, A., Palomino-Schätzlein, M., Abián, O., Velázquez-Campoy, A., Iovanna, J.L., (2020). A phosphorylation-induced switch in the nuclear localization sequence of the intrinsically disordered NUPR1 hampers binding to importin. *Biomolecules* **10**, 1313. https://doi.org/10.3390/biom10091313.
28. Cano, C.E., Hamidi, T., Sandi, M.J., Iovanna, J.L., (2011). Nupr-1: the Swiss knife of cancer. *J. Cell. Physiol.* **226**, 1439–1443. https://doi.org/10.1002/jcp.22324.
29. Goruppi, S., Iovanna, J.L., (2010). Stress-inducible protein p8 is involved in several physiological and pathological processes. *J. Biol. Chem.* **285**, 1577–1581. https://doi.org/10.1074/jbc.R109.080887.
30. Santofimia-Castaño, P., Rizzuti, B., Pey, A.L., Soubeyran, P., Vidal, M., Urrutia, R., Iovanna, J.L., Neira, J.L., (2017). Intrinsically disordered chromatin protein NUPR1 binds to the C-terminal region of Polycomb RING1B. *PNAS* **114**, E6332–E6341. https://doi.org/10.1073/pnas.1619932114.
31. Santofimia-Castaño, P., Rizzuti, B., Pey, A.L., Fárez-Vidal, M.E., Iovanna, J.L., Neira, J.L., (2021). Intrinsically disordered protein NUPR1 binds to the armadillo-repeat domain of Plakophilin 1. *Int. J. Biol. Macromol.* **170**, 549–560. https://doi.org/10.1016/j.ijbiomac.2020.12.193.
32. Santofimia-Castaño, P., Huang, C., Liu, X., Xia, Y., Audebert, S., Camoin, L., Peng, L., Lomberk, G., et al., (2022). NUPR1 protects against hyperPARylation-dependent cell death. *Commun. Biol.* **5**, 732. https://doi.org/10.1038/s42003-022-03705-1.
33. Malicet, C., Giroux, V., Vasseur, S., Dagorn, J.C., Neira, J. L., Iovanna, J.L., (2006). Regulation of apoptosis by the p8/prothymosin alpha complex. *PNAS* **103**, 2671–2676. https://doi.org/10.1073/pnas.0508955103.
34. Lopez, M.B., Garcia, M.N., Grasso, D., Bintz, J., Molejon, M.I., Velez, G., Lomberk, G., Neira, J.L., et al., (2015). Functional Characterization of Nupr1L, A Novel p53-Regulated Isoform of the High-Mobility Group (HMG)-Related Protumoral Protein Nupr1. *J. Cell. Physiol.* **230**, 2936–2950. https://doi.org/10.1002/jcp.25022.
35. Neira, J.L., Rizzuti, B., Jiménez-Alesanco, A., Abián, O., Velázquez-Campoy, A., Iovanna, J.L., (2020). The paralogue of the intrinsically disordered nuclear protein 1 has a nuclear localization sequence that binds to Human Importin α3. *Int. J. Mol. Sci.* **21**, 7428. https://doi.org/10.3390/ijms21197428.
36. Urrutia, R., Velez, G., Lin, M., Lomberk, G., Neira, J.L., Iovanna, J., (2014). Evidence supporting the existence of a NUPR1-like family of helix-loop-helix chromatin proteins related to, yet distinct from, AT hook-containing HMG proteins. *J. Mol. Model.* **20**, 2357. https://doi.org/10.1007/s00894-014-2357-7.
37. Neira, J.L., López, M.B., Sevilla, P., Rizzuti, B., Cámara-Artigas, A., Vidal, M., Iovanna, J.L., (2018). The chromatin nuclear protein NUPR1L is intrinsically disordered and binds to the same proteins as its paralogue. *Biochem. J.* **475**, 2271–2291. https://doi.org/10.1042/BCJ20180365.
38. Lis, S., Costa, M., (2022). The role of NUPR1 in response to stress and cancer development. *Tox. App. Pharmacol.* **454**, https://doi.org/10.1016/j.taap.2022.116244 116244.
39. Chang, X., Fang, K., (2010). PADI4 and tumorigenesis. *Cancer Cell Int.* **10**, 7. https://doi.org/10.1186/1475-2867-10-7.
40. Fuhrmann, J., Clancy, K.W., Thompson, P.R., (2015). Chemical biology of protein arginine modifications in epigenetic regulation. *Chem. Rev.* **115**, 5413–5461. https://doi.org/10.1021/acs.chemrev.5b00003.
41. Mondal, S., Thompson, P.R., (2021). Chemical biology of protein citrullination by the protein arginine deiminases. *Cur. Opin. Strcut. Biol.* **63**, 19–27. https://doi.org/10.1016/j.cbpa.2021.01.010.
42. Miskei, M., Antal, C., Fuxreiter, M., (2017). FuzDB: Database of fuzzy complexes, a tool to develop stochastic structure-function relationships for protein complexes and higher order assemblies. *Nucleic Acids Res.* **45**, D228–D235. https://doi.org/10.1093/nar/gkw1019.
43. Horikoshi, N., Tachiwana, H., Saito, K., Osakabe, A., Sato, M., Yamada, M., Akashi, S., Nishimura, Y., et al., (2011). Structural and biochemical analyses of the human PAD4 variant encoded by a functional haplotype gene. *Acta Crystallogr.* **D67**, 112–118. https://doi.org/10.1107/S0907444910051711.

44. Rai, R.K., Tripathi, P., Sinha, N., (2009). Quantification of metabolites from two-dimensional nuclear magnetic resonance spectroscopy: Application to human urine samples. *Anal. Chem.* **81**, 10232–10238. https://doi.org/10.1021/ac902405z.
45. Pastore, A., Temussi, P.A., (2017). The emperor's new clothes: Myths and truths of in-cell NMR. *Arch. Biochem. Biophys.* **628**, 114–122. https://doi.org/10.1016/j.abb.2017.02.008.
46. Neira, J.L., Bintz, J., Arruebo, M., Rizzuti, B., Bonacci, T., Vega, S., Lanas, A., Velázquez-Campoy, A., et al., (2017). Identification of a drug targeting an intrinsically disordered protein involved in pancreatic adenocarcinoma. *Sci. Rep.* **7**, 39732. https://doi.org/10.1038/srep39732.
47. Santofimia-Castaño, P., Xia, Y., Lan, W., Zhou, Z., Huang, C., Peng, L., Soubeyran, P., Velázquez-Campoy, A., et al., (2019). Ligand-based design identifies a potent NUPR1 inhibitor exerting anticancer activity via necroptosis. *J. Clin. Inves.* **129**, 2500–2513. https://doi.org/10.1172/JCI127223.
48. Rizzuti, B., Lan, W., Santofimia-Castaño, P., Zhou, Z., Velázquez-Campoy, A., Abián, O., Peng, L., Neira, J.L., et al., (2021). Design of inhibitors of the intrinsically disordered protein NUPR1: balance between drug affinity and target function. *Biomolecules* **11**, 1453. https://doi.org/10.3390/biom11101453.
49. Ventero, M.P., Fuentes-Baile, M., Quereda, C., Perez-Valeciano, E., Alenda, C., Garcia-Morales, P., Esposito, D., Dorado, P., et al., (2019). Radiotherapy resistance acquisition in Glioblastoma. Role of SOCS1 and SOCS3. *PLoS One* **14**, e0212581. https://doi.org/10.1371/journal.pone.0212581.
50. Fuentes-Baile, M., Pérez-Valenciano, E., de Garcia-Morales, P., Juan Romero, C., Bello-Gil, D., Barbera, V. M., Rodríguez-Lescure, A., Sanz, J.M., et al., (2021). CLytA-DAAO chimeric enzyme bound to magnetic nanoparticles. A new therapeutical approach for cancer patients? *Int. J. Mol. Sci.* **22**, 1477. https://doi.org/10.3390/ijms22031477.
51. Sekhar, A., Kay, L.E., (2013). NMR paves the way for atomic level descriptions of sparsely populated, transiently formed biomolecular conformers. *PNAS* **110**, 12867–12874. https://doi.org/10.1073/pnas.1305688110.
52. Fusco, G., De Simone, A., Gopinath, T., Vostrikov, V., Vendruscolo, M., Dobson, C.M., Veglia, G., (2014). Direct observation of the three regions in α-synuclein that determine its membrane-bound behaviour. *Nat. Commun.* **5**, 3827. https://doi.org/10.1038/ncomms4827.
53. Arbesu, M., Maffei, M., Cordeiro, T.N., Teixeira, J.M.C., Pérez, Y., Bernardo, P., Roche, S., Pons, M., (2017). The unique domain forms a fuzzy intramolecular complex in SRC family kinases. *Structure* **25**, 630–640. https://doi.org/10.1016/j.str.2017.02.011.
54. Borkosky, S.S., Camporeale, G., Chemes, L.B., Risso, M., Noval, M.G., Sánchez, I.E., Alonso, L.G., De Prat Gay, G., (2017). Hidden structural codes in protein intrinsic disorder. *Biochemistry* **56**, 5560–5569. https://doi.org/10.1021/acs.biochem.7b00721.
55. Mittag, T., Kay, L.E., Forman-Kay, J.D., (2010). Protein dynamics and conformational disorder in molecular recognition. *J. Mol. Recognit.* **23**, 105–116. https://doi.org/10.1002/jmr.961.
56. Freibrger, M.L., Wolynes, P.G., Ferreiro, D.U., Fuxreiter, M., (2021). Frustration in fuzzy protein complexes leads to interaction versatility. *J. Phys. Chem.* **125**, 2513–2520. https://doi.org/10.1021/acs.jpcb.0c11068.
57. Murphy, A., Costa, M., (2020). Nuclear protein 1 imparts oncogenic potential and chemotherapeutic resistance in cancer. *Cancer Lett.* **494**, 132–141. https://doi.org/10.1016/j.canlet.2020.08.019.
58. Malicent, C., Lesavre, N., Vasseur, S., Iovanna, J.L., (2003). p8 inhibits the growth of human pancreatic cancer cells and its expression is induced through pathways involved in growth inhibition and repressed by factors promoting cell growth. *Mol. Cancer* **2**, 37. https://doi.org/10.1186/1476-4598-2-37.
59. Chang, X., Han, J., Pang, L., Zhao, Y., Yang, Y., Shan, Z., (2009). Increased PADI4 expression in blood and tissues of patient with malignant tumors. *BMC Cancer* **9**, 40. https://doi.org/10.1186/1471-2407-9-40.
60. Moshkovic, N., Ochoa, H.J., Tang, B., Yang, H.H., Yang, Y., Huang, J., Lee, M.P., Wakefield, L.M., (2020). Peptidylarginine deiminase IV regulates breast cancer stem cells vi a novel tumor cell-autonomous suppressor role. *Cancer Res.* **80**, 2125–2137. https://doi.org/10.1158/0008-5472.CAN-19-3018.
61. Li, P., Yao, H., Zhang, Z., Li, M., Luo, Y., Thompson, P.R., Glimour, D.S., Wang, Y., (2008). Regulation of p53 target gene expression by peptidyl-arginine deiminase 4. *Mol. Cell Biol.* **28**, 4745–4758. https://doi.org/10.1128/MCB.01747-07.
62. Guo, Q., Fast, W., (2011). Citrullination of inhibitor growth 4 (ING4) by peptidylarginine deminase 4 (PAD4) disrupts the interaction between ING4 and p53. *J. Biol. Chem.* **286**, 17069–17078. https://doi.org/10.1074/jbc.M111.230961.
63. Darrah, E., Giles, J.T., Ols, M.L., Bull, H.G., Andrade, F., Rosen, A., (2013). Erosive rheumatoid arthritis is associated with antibodies that activate PAD4 by increasing calcium sensitivity. *Sci. Transl. Med.* **5**, 186ra65. https://doi.org/10.1126/scitranslmed.3005370.
64. Dong, S., Zhang, Z., Takahara, H., (2007). Estrogen-enhanced peptidylarginine deiminase type IV gene (PADI4) expression in MCF-7 cells is mediated by estrogen receptor-α-promoted transfactors activator protein-1, nuclear factor-Y and Sp1. *Mol. Endocrinol.* **21**, 1617–1629. https://doi.org/10.1210/me.2006-0550.
65. Gironella, M., Malicet, C., Cano, C., Sandi, M.J., Hamidi, T., Tauil, R.M.N., Baston, M., Valaco, P., et al., (2009). p8/NUPR1 regulates DNA-repair activity after double-strand gamma irradiation-induced DNA-damage. *J. Cell. Physiol.* **221**, 594–602. https://doi.org/10.1002/jcp.21889.
66. Ree, A.H., Tvermyr, M., Engebraaten, O., Rooman, M., Røsok, O., Hovig, E., MezaZepeda, L.A., Bruland, O.S., et al., (1999). Expression of a novel factor in human breast cancer cells with metastatic potential. *Cancer Res.* **59**, 4675–4680.
67. Stadler, S.C., Vicent, C.T., Fedorov, V.D., Patsialou, A., Cherrington, B.D., Wakshlag, J.J., Mohanan, S., Zee, B.M., et al., (2013). Dysregulation of PADI4-mediated citrullination of nuclear GSK-3β activates TGF-beta signaling and induces epithelial-to-mesenchymal transition in breast cancer cells. *PNAS* **110**, 11851–11856. https://doi.org/10.1073/pnas.1308362110.
68. Gill, S.C., von Hippel, P.H., (1989). Calculation of protein extinction coefficients from amino acid sequence data. *Anal. Biochem.* **182**, 319–326. https://doi.org/10.1016/0003-2697(89)90602-7.

69. Neira, J.L., Hornos, F., Bacarizo, J., Cámara-Artigas, A., Gómez, J., (2017). The monomeric species of the regulatory domain of tyrosine hydroxylase has a low conformational stability. *Biochemistry* **55**, 3418–3431. https://doi.org/10.1021/acs.biochem.6b00135.
70. Birdsall, B., King, R.W., Wheeler, M.R., Lewis Jr., C.A., Goode, S., Dunlap, R.B., Roberts, G.C., (1983). Correction for light absorption in fluorescence studies of protein-ligand interactions. *Anal. Biochem.* **132**, 353–361. https://doi.org/10.1016/0003-2697(83)90020-9.
71. Beckett, D., (2011). Measurement and analysis of equilibrium binding titrations: a beginner's guide. *Methods Enzymol.* **488**, 1–16. https://doi.org/10.1016/B978-0-12-381268-1.00001-X.
72. Royer, C.A., Scarlatta, S.F., (2008). Fluorescence approaches to quantifying biomolecular interactions. *Methods Enzymol.* **450**, 79–106. https://doi.org/10.1016/S0076-6879(08)03405-8.
73. Cavanagh, J.F., Wayne, J., Palmer III, A.G., Skelton, N.J., (1996). Protein NMR Spectroscopy: Principles and Practice. Academic Press, San Diego.
74. Bodenhausen, G., Ruben, D., (1980). Natural abundance nitrogen-15 NMR by enhanced heteronuclear spectroscopy. *Chem. Phys. Lett.* **69**, 185–189.
75. Bonucci, A., Palomino-Schätzlein, M., Malo de Molina, P., Arbe, A., Pierattelli, R., Rizzuti, B., Iovanna, J.L., Neira, J. L., (2021). Crowding effects on the structure and dynamics of the intrinsically disordered nuclear chromatin protein NUPR1. *Front. Mol. Biosci.* **8**, https://doi.org/10.3389/fmolb.2021.684622 684622.
76. Santofimia-Castaño, P., Rizzuti, B., Abián, O., Velázquez-Campoy, A., Iovanna, J.L., Neira, J.L., (2018). Amphipathic helical peptides hamper protein-protein interactions of the intrinsically disordered chromatin nuclear protein 1 (NUPR1). *Biochim. Biophys. Acta Gen. Sub.* **1862**, 1283–1295. https://doi.org/10.1016/j.bbagen.2018.03.009.
77. Trott, O., Olson, A.J., (2010). AutoDock Vina: Improving the speed and accuracy of docking with a new scoring function, efficient optimization, and multithreading. *J. Comput. Chem.* **31**, 455–461. https://doi.org/10.1002/jcc.21334.
78. Grande, F., Rizzuti, B., Occhiuzzi, M.A., Ioele, G., Casacchia, T., Gelmini, F., Guzzi, R., Garofalo, A., et al., (2018). Identification by molecular docking of homoisoflavones from *Leopoldia comosa* as ligands of estrogen receptors. *Molecules* **23**, 894. https://doi.org/10.3390/molecules23040894.